

Attachment of Lead Wires to Thin Film Thermocouples Mounted on High Temperature Materials Using the Parallel Gap Welding Process

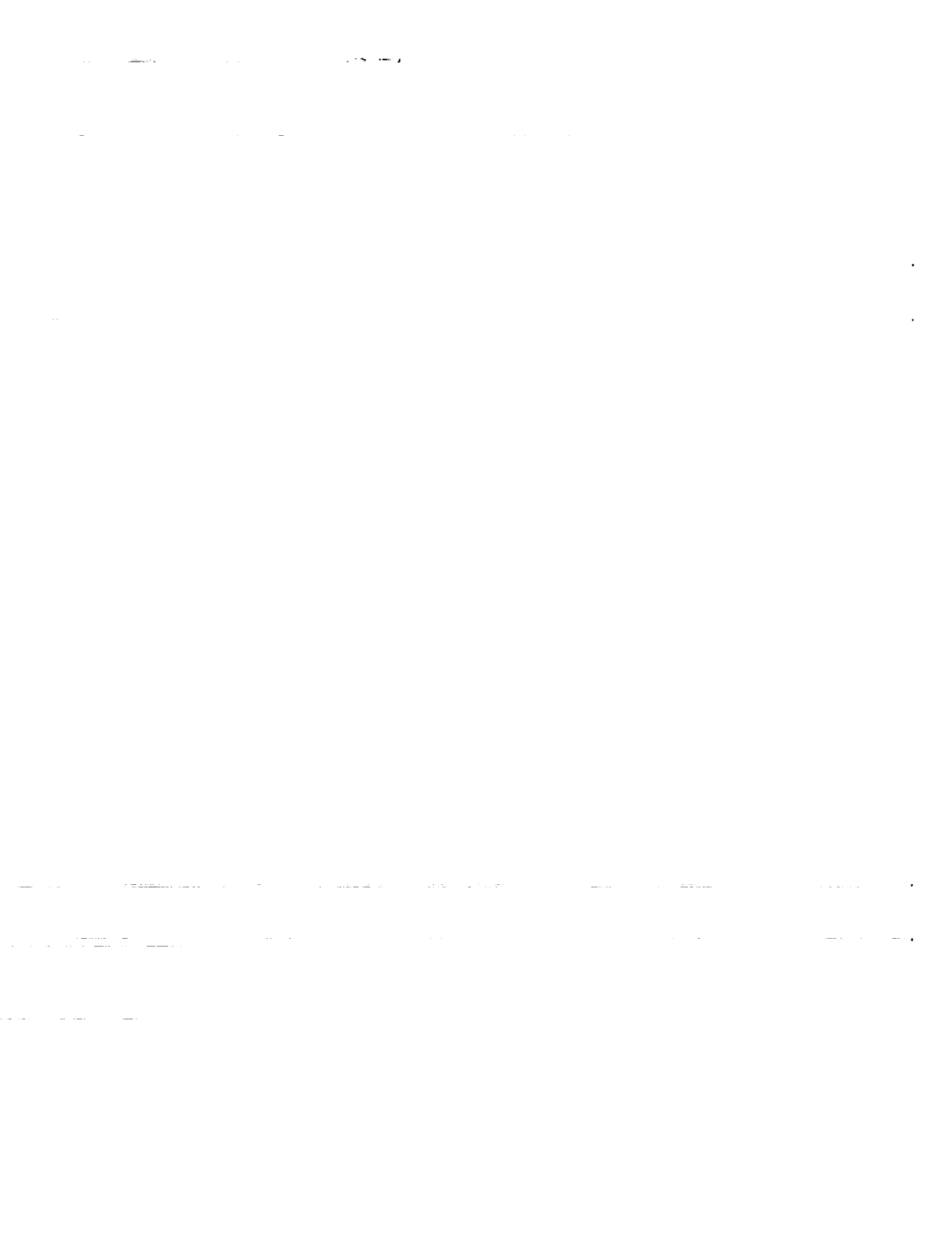
Raymond Holanda and Walter S. Kim
Lewis Research Center
Cleveland, Ohio

Eric Pencil and Mary Groth
University of Cincinnati
Cincinnati, Ohio

Gerald A. Danzey
Lewis Research Center
Cleveland, Ohio

Prepared for the
177th Meeting of the Electrochemical Society
Montreal, Quebec, Canada, May 6-11, 1990





ATTACHMENT OF LEAD WIRES TO THIN FILM THERMOCOUPLES MOUNTED ON
HIGH TEMPERATURE MATERIALS USING THE
PARALLEL GAP WELDING PROCESS

Raymond Holanda and Walter S. Kim
National Aeronautics and Space Administration
Lewis Research Center
Cleveland, Ohio 44135

Eric Pencil* and Mary Groth*
University of Cincinnati
Cincinnati, Ohio 45221

Gerald A. Danzey
National Aeronautics and Space Administration
Lewis Research Center
Cleveland, Ohio 44135

SUMMARY

Parallel gap resistance welding was used to attach lead wires to sputtered thin film sensors. Ranges of optimum welding parameters to produce an acceptable weld were determined. The thin film sensors were Pt13Rh/Pt thermocouples; they were mounted on substrates of MCrAlY-coated superalloys, aluminum oxide, silicon carbide, and silicon nitride. The wires were 76 μm diameter Pt and Pt13Rh, and both round and preflattened wires were used. The entire sensor system is designed to be used on aircraft engine parts. These sensor systems, including the thin-film-to-lead-wire connections, have been tested to 1000 °C.

REVIEW OF PREVIOUS WORK

In recent years, thin film sensors have been used for temperature and heat flux measurements on high temperature materials. These sensors have been used in applications to 1000 °C on metal parts, and even higher temperatures are expected as ceramic components are developed for advanced propulsion systems. One necessary and critical part of these sensor systems is a reliable thin-film-to-lead-wire junction to transfer the sensor signal from the engine component. Depending on the design of the component and the measurement required, this connection could be exposed to a temperature level at or near the temperature being measured.

Several different methods have been used to fabricate thin-film-to-lead-wire junctions for these applications. A thermocompression bond was used to attach lead wires to thin film thermocouples on turbine blades (refs. 1 to 4). The lead wires were clamped to the film and heated at 865 °C for at least 4 hr to produce a diffusion-bonded junction rugged enough to survive on a jet engine rotor. Pt and Pt10Rh films and wires were used. The chief drawback of the thermocompression bonding process is the time consumed to make the connections.

*Student Co-op at NASA Lewis Research Center.

A second method used to connect lead wires to thin films was with conductive paste. A Pt/Pd/Au conductive paste was used to attach lead wires to a Pt and Pt10Rh thin film thermocouple (refs. 5 and 6). Maximum use temperature for the connection was found to be about 800 °C, and a Pt-based conductive paste was found that could withstand higher temperatures (>1000 °C). A conductive compound used in the electronic industry for thick-film gold circuits connected lead wires to Platine1 thin film thermocouples for jet engine turbine blade temperature measurement (refs. 8 and 9). One problem with these pastes is that they must be fired at high temperature in an oven for a specified period of time (up to 1 hr). Another problem is the introduction into the thermocouple circuit of a material that has a composition different from the thermoelement.

In another method, thin-film-to-lead-wire connections were made for a flat plate heat transfer experiment by encapsulating the lead wires in flame-sprayed insulating material and sputtering the thin film sensors through this porous layer (ref. 7). The wire and thin film were both nickel and the maximum use temperature of the connection was about 600 °C. The difficulty with this connection is that the flame-sprayed material thickness must be very carefully controlled in the area of the lead wire connection to be able to sputter through it.

A fourth method used to attach lead wires to thin films on high temperature materials was with the use of a parallel gap welder. Lead wires were attached to thin film thermocouples on space shuttle main engine blades for temperature measurement to 1000 °C (ref. 10). Pt10Rh/Pt thin films and lead wires were used. These connections survived thermal cycling between 1000 °C and liquid nitrogen temperatures. The parallel gap welding process was also used to attach lead wires to thin films that were on a heat transfer plug mounted in a ceramic insulated, low-heat rejection diesel engine (refs. 11 and 12). The Pt13Rh/Pt thin films were sputter-deposited on plasma-sprayed ZrO₂ ceramic material and exposed to temperatures of 700 °C in the engine.

The advantages of the parallel-gap welding process for thin-film-to-lead-wire connections are: the instantaneous formation of the bond; the introduction of no additional material into the thermocouple circuit; and the ability of the connection to withstand a temperature level as high as the thin film thermocouple itself. However, the welding schedules vary for each combination of film, wire, and substrate material, and this information needs to be determined for a wider range of materials. Therefore, a program evolved at this laboratory to apply this process to thin film thermocouples on high temperature materials. An analysis of this data was then performed.

Thin film thermocouples were applied to MCrAlY-coated superalloys as well as Al₂O₃, Si₃N₄, and SiC ceramic materials. Each substrate material requires a unique approach to the thin film sensor fabrication process. Figure 1 illustrates these differences. The MCrAlY-coated superalloys and SiC require an electrically insulating layer between the base material and the sensor while Si₃N₄ and Al₂O₃ do not. The insulating layer consists of a two-step process of thermally grown and sputter-deposited oxides to produce pore-free electrical isolation of the sensor.

APPARATUS AND EXPERIMENTAL PROCEDURE

The parallel gap welder is shown in figure 2. It is a resistance welding device with a pair of parallel welding electrodes. For application to thin-film-to-lead-wire connections, the lead wire is positioned on the thin film and the electrodes press the lead wire against the thin film with a preselected force (fig. 3). The current passes from one electrode, through the part to be welded, and back through the other electrode. The user has control of the variables of weld voltage, weld time duration, electrode force, and electrode spacing.

The parallel gap welder uses a constant voltage power supply, which delivers a current output (0 to 600 A) that varies to maintain a constant weld voltage. The power supply produces a uniform square wave dc pulse output. Weld voltage is controllable from 0.01 to 1.99 V; time of the weld pulse is controllable from 1 to 9900 msec; electrode force is adjustable from 60 to 1000 g; and electrode gap is adjustable from 0 to 1 mm (0 to 0.040 in.). The electrodes are made of a molybdenum-molybdenum carbide alloy. The actual values of the welding parameters used in the tests were as follows: the weld voltage was varied from 0.90 to 1.99 V; the time of the weld pulse varied from 5 to 100 msec; the electrode force was varied from 180 to 975 g. These ranges were chosen either because they represented the maximum range of a parameter or because no further improvement in results was noted by further change in a parameter. The gap size was chosen to be 1.5 times the wire diameter (125 μm) based on manufacturer's recommendation and trial experimentation.

In order to clean the electrode tips, the electrode gap is opened to the thickness of the abrading material. Both the tip and the inside of the electrodes are cleaned with 600 grit sandpaper using a circular motion. After sanding, all debris is removed by dusting with pressurized nitrogen gas. The electrodes are examined under the microscope to determine if all loose debris has been removed. The next step in the preparation of this machine is the alignment of the electrodes. The tips of the electrodes must be parallel to each other as well as aligned in the vertical direction. The gap is set using feeler gauges between the tips of the electrodes.

Oxides that are present on the surface of the wire or film need to be removed before welding. This is accomplished with the use of 600 grit sandpaper. Organic contamination can also be present on the wire and film from handling and other sources. Wire and film surfaces are cleaned with alcohol as needed.

A simple and practical weld test procedure, well suited to thin-film-to-lead-wire connections, was used in this program. The test is a destructive pull test. Because of the weakness of the film shear strength compared to the strength of the wire, a destructive pull test on the weld results in a slug of film attached to the wire. If this slug of film is equal to or greater than wire diameter and at the same time shows no discoloration or excessive deformation of the materials, it is a successful weld. Lower power would attach little or no film and higher power would discolor and distort the materials. Scanning electron microscope pictures taken of the weld area prior to the destructive pull test were used to complete the qualitative evaluation of the weld connections.

Tests were conducted by trying several different combinations of the welding parameters for each combination of film and lead wire material with each substrate. Each combination was tested for a minimum of three attempts. A weld was determined to be acceptable if it was successful for a majority of the attempts. Success was determined from the destructive pull test and the scanning electron microscope photomicrographs.

Pt wires were attached to Pt films and Pt13Rh wires were attached to Pt13Rh films to create thermocouple circuits. The diameter of the wires was selected to be 76 μm (0.003 in.) because of the wide usage of this size. A flattened version of this wire was also used in which the 76 μm wire was pre-flattened to about 50 μm . Thin film sensors varied in thickness from 1 to 7 μm . These sensors were sputter-deposited on substrates of SiC, Si₃N₄, Al₂O₃, and two superalloy materials, MAR-M-200+Hf and MAR-M-246+Hf. The superalloys were coated with 75 to 125 μm of NiCoCrAlY. This is a standard protective coating used on superalloy components in the jet engine hot section (ref. 1). Oxide layers were thermally grown and sputter-deposited on the SiC and the NiCoCrAlY-coated superalloy to electrically insulate the thin film sensor from the substrate. Surface finish of the substrate materials at this point of the fabrication process were in the 0.1 to 1 μm (4 to 40 $\mu\text{in.}$) range, as measured with a stylus-type profilometer.

RESULTS AND DISCUSSION

Scanning electron micrographs were taken of a representative sample of welds during the testing process. Examples of good welds are shown in figure 4. A variety of unacceptable welds together with a description of the type of failure represented by each micrograph are shown in figure 5. From these tests, welding schedules were determined for each film and lead wire material with each substrate.

Figures 6 to 9 show the effect of weld voltage on weld quality for Pt and Pt13Rh thin-film-to-lead-wire connections on two superalloy substrate materials. Only round wire was used. The two superalloy materials were MAR-M-200+Hf and MAR-M-246+Hf coated with NiCoCrAlY, which is one of the standard MCrAlY protective coatings for hot section components in jet engines.

Figures 10 to 15 show the effect of weld voltage on weld quality for Pt and Pt13Rh thin-film-to-lead-wire connections on silicon nitride, silicon carbide, and aluminum oxide ceramic substrate materials. Both round and preflattened wire were used on silicon nitride and silicon carbide, while only round wire was used on aluminum oxide.

By combining the welding schedule data from all the different substrate materials, probability distributions were found for the welding parameters of force and time. The effect of weld quality vs time duration of the weld voltage pulse is shown in figure 16; the effect of weld quality versus electrode force is shown in figure 17.

To facilitate the analysis of the data, a table of property values was prepared for the materials used in these experiments (table I). Included are values for the substrate materials, wire and thin film materials, and any other coatings used in the fabrication of the sensor systems.

The voltage setting was the most important factor in the determination of weld quality. At a setting that was lower than necessary, there would only be a small weld or no weld at all. When the voltage was increased too much, the section of wire as well as the thin film would melt away. At even higher values the thin film would burn first followed by the substrate.

Substrate material had a strong effect on the amount of energy needed to weld. The required energy increased with an increase in the thermal conductivity of the substrate material (fig. 18). The figure plots the optimum weld voltage obtained from figures 6 to 15 against the thermal conductivity of the substrate material. The substrate thus acts as a heat sink, drawing energy away from the weld area. The superalloys and silicon carbide have a thin insulation layer between the thin film sensor and the substrate. This layer does not seem to have a significant retarding effect on the heat transfer. In addition, the superalloys have a much thicker deposition of NiCoCrAlY on their surface. However, this coating has a thermal conductivity about the same as the superalloy substrate itself and therefore would not alter the heat transfer rate.

The time setting is the other factor related to the energy present during the welding process. If the voltage was at the lower end of the acceptable range, then longer time durations were needed. On the other hand, if the voltage was at the high end of the acceptable range, then the welding times needed to be shortened. At the peak of the normal distribution of the voltage settings, a wide range of time settings would produce acceptable welds. The net effect of these time-related factors would be a skewed distribution in the curve of weld time duration versus weld quality. Figure 16 shows the distribution obtained for all connections made on all substrates. The highest percentage of successful welds was obtained in the 50 to 80 msec range.

Of the three welding parameters of the parallel gap welder, the simplest to understand was the force setting. The force required increased as the hardness of the wire increased. The optimum range for Pt was 400 to 850 g, while the range for Pt13Rh was 600 to 1000 g (fig. 17). Pt hardness is 40 (Brinell Hardness), while Pt13Rh is 100 (Brinell Hardness). If the applied force was lower than necessary, the wire would melt but not adhere to the thin film. In the case where the force used was higher than necessary, the wire would be crushed proportionally to this excessive pressure. If enough heat was present, the wire would adhere to the thin film under the electrode tips instead of under the gap. At extremely high force settings the wire would stick to the electrodes as well as to the thin film. This would cause damage to the weld as the electrodes were lifted.

Little difference was found between the weldability of the Pt and Pt13Rh connections. Despite the significant differences in their physical properties of thermal conductivity and electrical resistivity, the welding parameters needed to produce successful welds were about the same on most substrate materials. The only instance where the optimum value of the welding voltage differed by more than 20 percent between Pt and Pt13Rh was for the SiC substrate with round wire. It was thought that the presence of an oxide layer on the Pt13Rh might have an effect on these results. An attempt was made to remove this layer from the thin film by lightly sanding the surface with 600 grit sandpaper. This did not result in any change of the welding parameters for

Pt13Rh, so this extra step in the preparation was abandoned. Table II summarizes the results of figures 6 to 17 based on the optimum value of each welding parameter for each thin film and lead wire material on each substrate.

Placement of the wire in relation to the electrodes is crucial. The wire should be centered under the electrodes and perpendicular to the gap. Otherwise, the pivoting motion of the electrodes as they are brought into contact with the wire would cause the wire to roll. This in turn would damage the thin film. In order to avoid this problem, the use of preflattened wire was investigated. It was discovered that the optimum welding parameters did not change significantly with this ribbon-like material. Therefore, only a small range of voltage settings were investigated. One area of major improvement was that the flattened wire did not display the tendency to roll as the electrodes came down. However, the flattening process cold-worked the wire, causing it to become fragile. Care was needed to insure that the wire would not break with handling. This indicated that an additional annealing step should be used after the flattening process.

Surface roughness profiles were obtained with a stylus-type profilometer. Scans taken for each substrate material are shown in figure 19 along with calculated roughness values (R). Surface roughness varied over a wide range from $R = 0.1 \mu\text{m}$ for aluminum oxide to as much as $R = 1.0 \mu\text{m}$ for silicon nitride and the superalloys. Despite the wide variation in this parameter, surface roughness had negligible effect on the ability to perform successful thin-film-to-lead-wire connections using the parallel gap resistance welding process.

A typical profilometer scan measuring Pt and Pt13Rh film thicknesses is shown in figure 20. A study of the effects of film thickness was conducted using MAR-M-246+Hf. The thickness of the thin film did not interfere with the welding process when the thickness fell in the 3 to 7 μm range. In the case where the film thickness was 1 to 2 μm , welds could be obtained, but they were more fragile and easily broken. Additional experimentation with silicon nitride substrates verified this finding.

Insofar as reliability is concerned, the parallel gap welder is very sensitive to the alignment of the electrodes. Great care is needed to set these electrodes parallel to each other. With the wide scope of this project, a large number of welds were made with the same set of electrodes. As a result, the tips were cleaned numerous times with 600 grit sandpaper. This amount of sanding changed the shape of the electrode tips. Caution is advised when using this equipment for such a large quantity of welds. Electrode maintenance is a factor in the consistency of the equipment performance that each individual user must evaluate.

CONCLUSIONS

Parallel gap welding was used to attach Pt and Pt13Rh lead wires to Pt and Pt13Rh sputtered thin film sensors to form thermocouple circuits. The thin films were mounted on superalloy and ceramic substrates for use in aircraft engine applications to 1000 °C or more. The superalloys were MAR-M-200+Hf and MAR-M-246+Hf, both coated with MCrAlY. The ceramics were SiC, Si₃N₄, and Al₂O₃.

Welding parameters of voltage, force, and time duration were determined for each wire and thin film combination on each substrate material to obtain successful welds. Optimum weld voltage ranged from 1.0 to 1.9 V, with increasing voltage required for increasing substrate thermal conductivity. Optimum time duration ranged from 20 to 80 msec. Optimum applied force ranged from 400 to 850 g for Pt to 600 to 1000 g for Pt13Rh and increased with increasing wire hardness.

Surface finish of substrates used in this investigation varied from about 0.1 to 1 μm . Film thicknesses of the Pt and Pt13Rh varied from 1 to 7 μm , with the most consistent results obtained in the 3 to 7 μm range.

REFERENCES

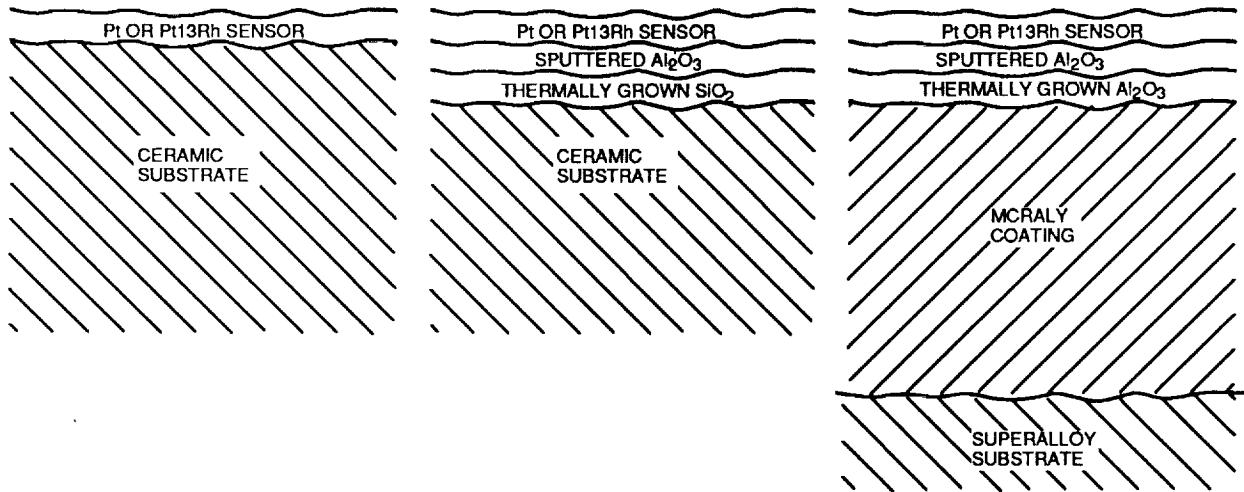
1. H.P. Grant, and J.S. Przybyszewski, "Thin Film Temperature Sensor," NASA-CR-159782 (1980).
2. J.S. Przybyszewski, and R.G. Claing, "Joining Lead Wires to Thin Platinum Alloy Films," U.S. Pat. 4,402,447 (1980).
3. H.P. Grant, J.S. Przybyszewski, and R.G. Claing, "Turbine Blade Temperature Measurements Using Thin Film Temperature Sensors," NASA CR-165201 (1981).
4. H.P. Grant, J.S. Przybyszewski, R.G. Claing, and W.L. Anderson, "Thin Film Temperature Sensors. Phase III," NASA CR-165476 (1982).
5. R.C. Budhani, S. Prakash, and R.F. Bunshah, J. Vac. Sci. Technol. A, **4**, 2609, (1986).
6. S. Prakash, "Thin Film Temperature Sensors for Gas Turbines," Ph.D. Thesis, UCLA, Los Angeles, CA, (1987).
7. C.H. Liebert, R. Holanda, S.A. Hippensteele, and C.A. Andracchio, J. Eng. Gas Turbines Power, **107**, 938 (1985).
8. J.C. Godefroy, D. Francois, C. Gageant, F. Miniere, and M. Portat, in International Conference on Metallurgical Coatings, San Diego, CA, Apr. 7-11, 1986, Paper No. 1986-28 (1986).
9. J.C. Godefroy, C. Gageant, D. Francois, and M. Portat, J. Vac. Sci. Technol. A, **5**, 2917 (1987).
10. W.S. Kim, "Progress on Thin Film Sensors for Space Technology," in "Structural Integrity and Durability of Reusable Space Propulsion Systems," NASA CP-2471, pp. 39-42 (1987).
11. W.S. Kim, and R.F. Barrows, "Prototype Thin Film Thermocouple/Heat-Flux Sensor for a Ceramic-Insulated Diesel Engine," NASA TM-100798 (1988).
12. K.G. Krieder, and M. Yust, in Proceedings of AIChE Symposium on Sensors Meeting (1988).

TABLE I. - PHYSICAL PROPERTY VALUES FOR THE MATERIALS USED IN THESE EXPERIMENTS

	Density, gm/cm ³	Thermal conductivity, k, W/mK	Electrical resistivity		Brinell hardness		Melting point, °C
			Ω-cm	μΩ-cm	Annealed	Cold-worked	
Si ₃ N ₄	3.28	30	10 ¹⁴	---	---	---	1900
SiC	3.3	125	10 ¹⁶	---	---	---	2700
Al ₂ O ₃	4.0	20	10 ¹⁴	---	---	---	2040
SiO ₂	2.2	2	10 ¹⁴	---	---	---	1700
Pt	21.5	70	----	10	40	87	1769
Pt13Rh	19.6	35	----	20	100	175	1860
MAR-M-200+Hf							
At 25 °C	8.5	13	----	130	---	---	1350
At 400 °C	----	15	----	---	---	---	----
MAR-M-246+Hf							
At 400 °C	----	17	----	---	---	---	----
NiCoCrAlY	----	20	----	---	---	---	----

TABLE II. - OPTIMUM VALUES OF PARALLEL GAP WELDING
PARAMETERS FOR Pt AND Pt13Rh THIN-FILM-TO-
LEAD-WIRE CONNECTIONS ON SUPERALLOY
AND CERAMIC MATERIALS

Optimum voltage, V				
	Round wire		Preflattened wire	
	Pt	Pt13Rh	Pt	Pt13Rh
MAR-M-246+Hf	1.20	1.10	----	----
MAR-M-200+Hf	1.10	1.30	----	----
Silicon nitride	1.40	1.30	1.40	1.40
Silicon carbide	1.50	1.90	1.80	1.90
Aluminum oxide	1.10	1.00	----	----
Optimum force, g (>50 percent success)				
All substrate materials	Round and preflattened wire			
	Pt		Pt13Rh	
	400 to 850		600 to 1000	
Optimum time duration, msec (>50 percent success)				
All substrate materials	Round and preflattened wire			
	Pt		Pt13Rh	
	20 to 80		20 to 80	



(a) Silicon nitride or aluminum oxide.

(b) Silicon carbide.

(c) MAR-M-200+Hf or MAR-M-246+Hf.

Figure 1. - Schematic diagram of thin film temperature sensors on ceramic and superalloy substrates.

ORIGINAL PAGE
BLACK AND WHITE PHOTOGRAPH

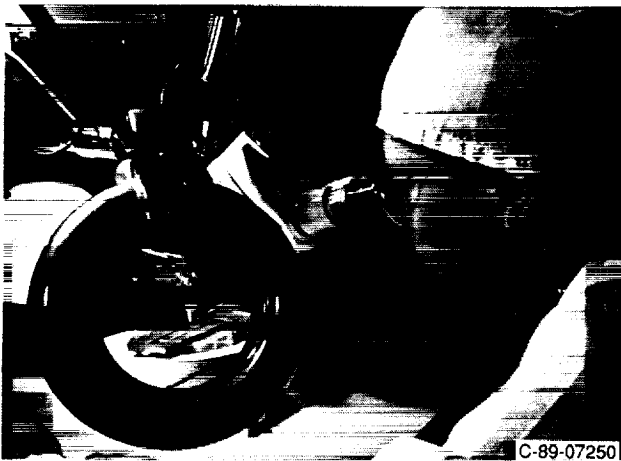


Figure 2. - Photograph of parallel gap resistance welding equipment showing a demonstration of a thin-film-to-lead-wire connection.

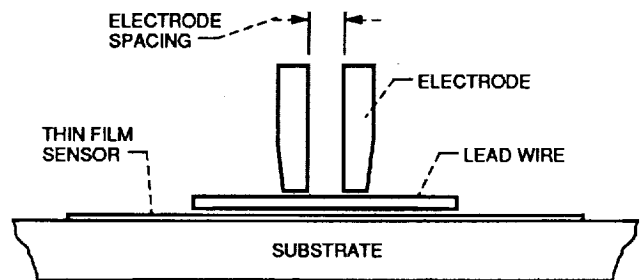


Figure 3. - Schematic drawing of parallel gap resistance welding equipment showing the position of the electrodes in the process of fabricating a thin-film-to-lead-wire connection.

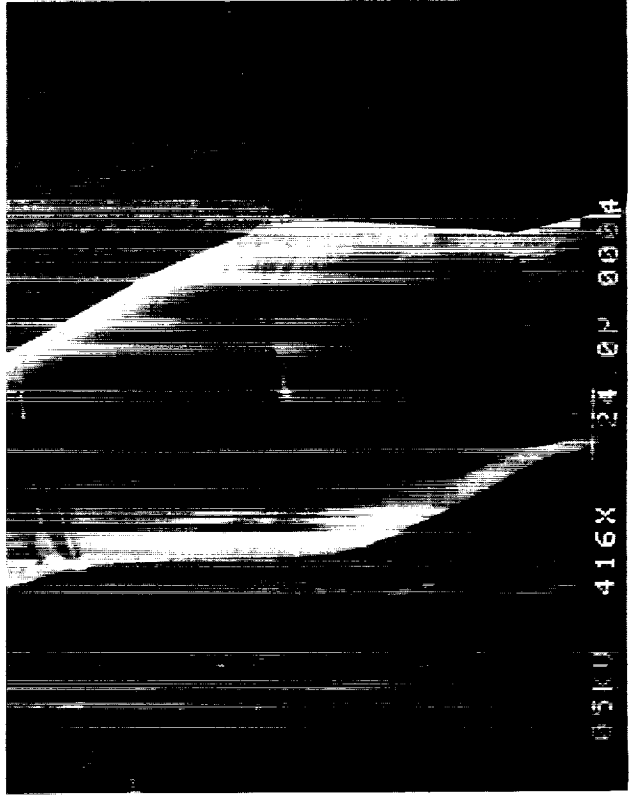
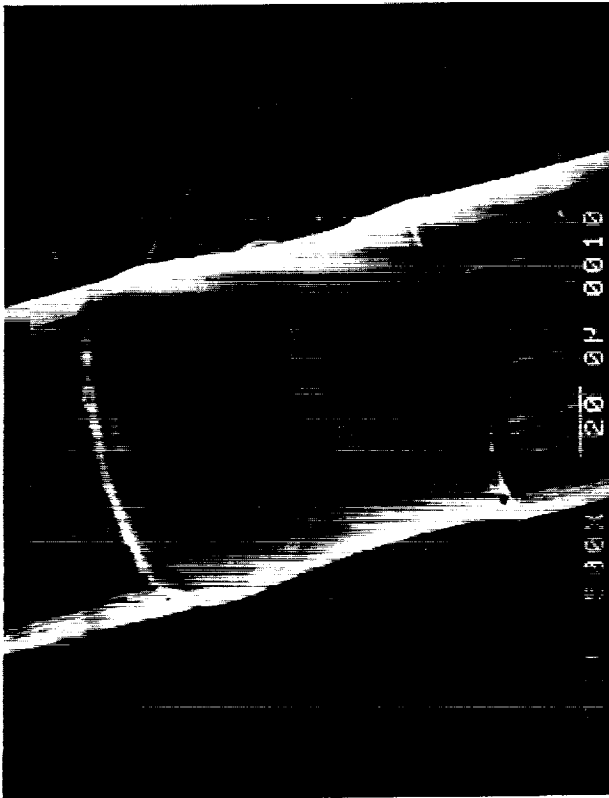
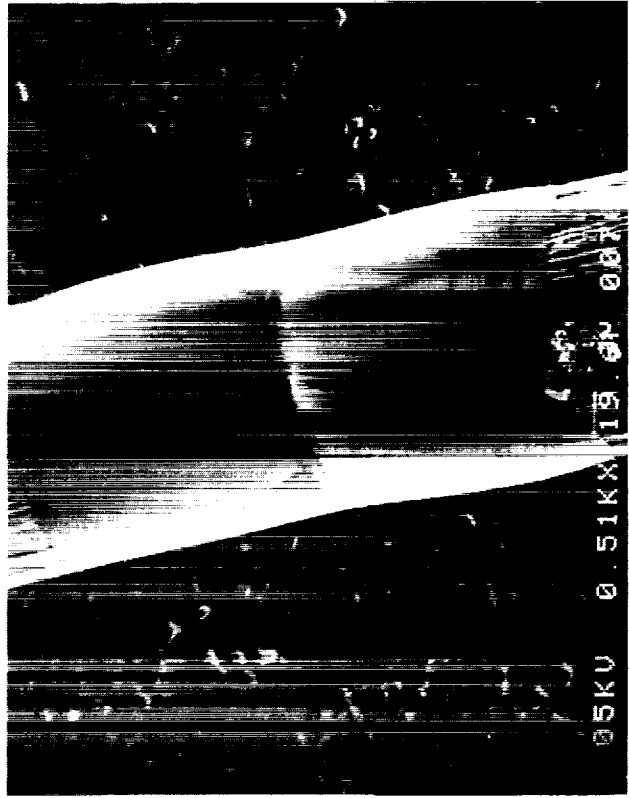
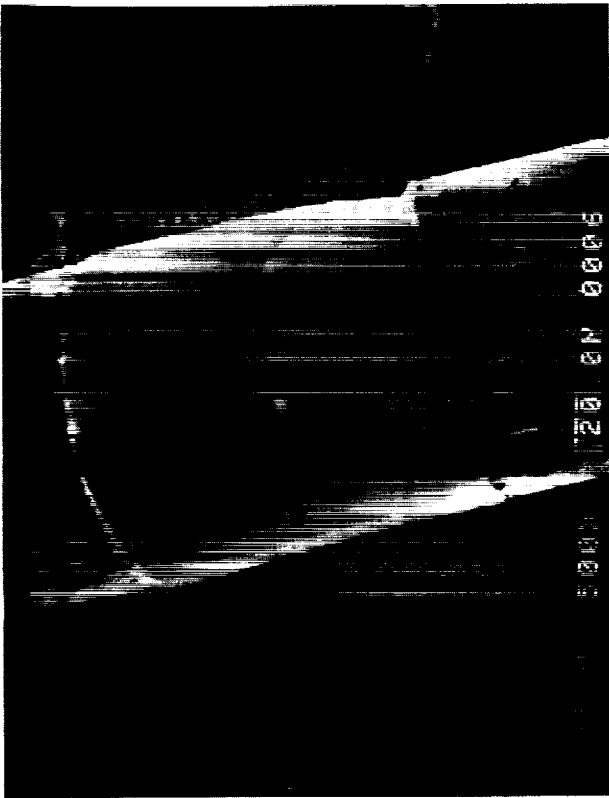
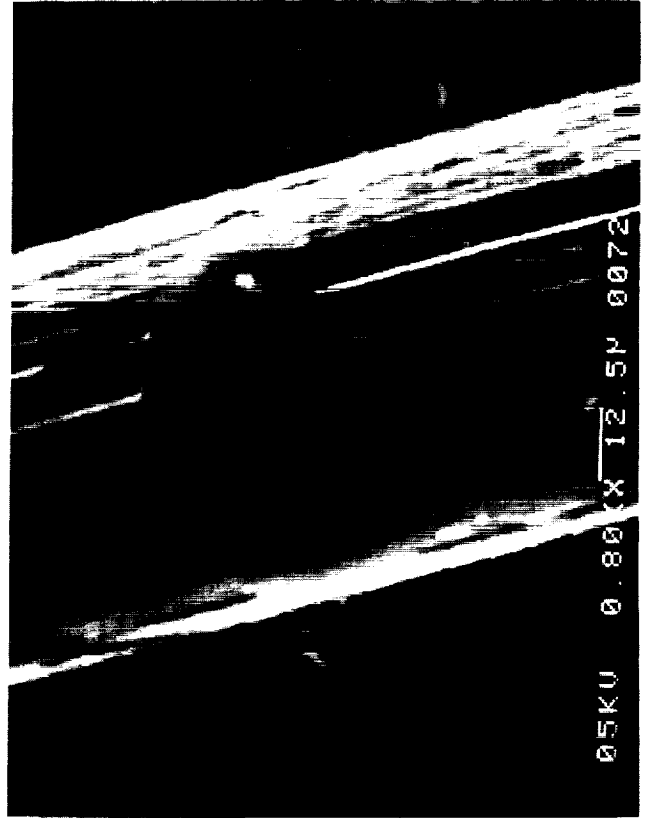


Figure 4. - Scanning electron microscope pictures showing examples of successful thin-film-to-lead-wire connections.



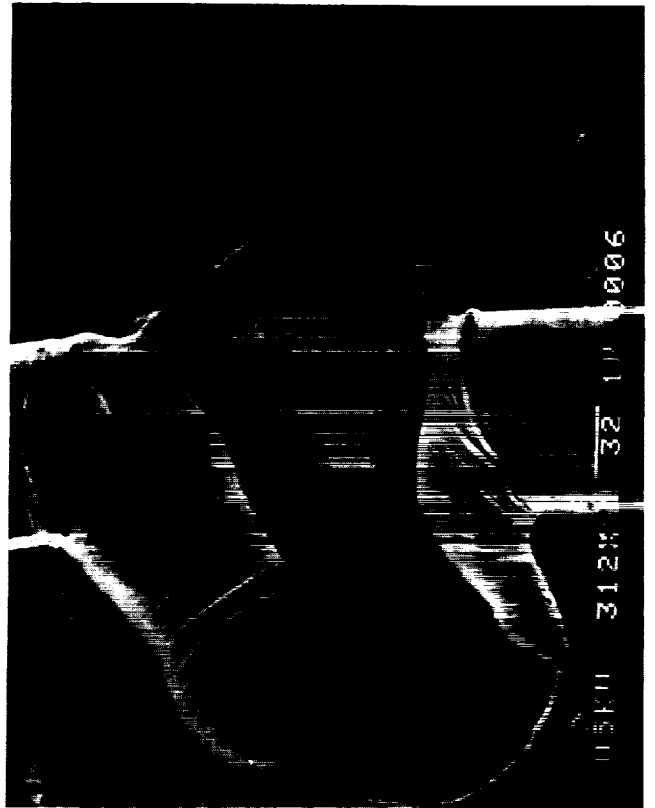
(a) Weak or Insufficient weld.



(b) Weak or Insufficient weld.

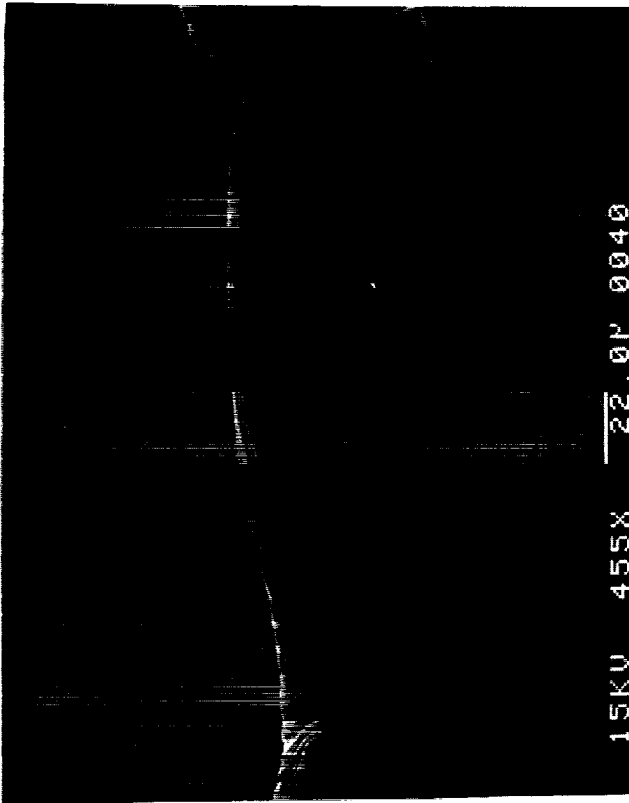


(c) Burnt film and blow hole.



(d) Burnt film and burnt substrate.

Figure 5. - Scanning electron microscope pictures showing examples of unsuccessful thin-film-to-lead-wire connections.



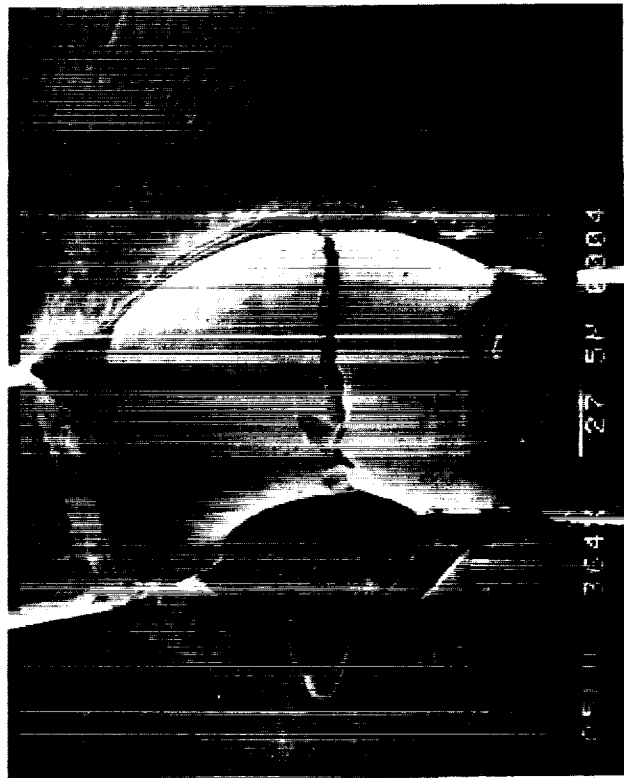
(e) Extreme wire melting.



(g) Burnt film and blow hole.



(f) Extreme wire melting.



(h) Cracked weld.

Figure 5. - Concluded.

ORIGINAL PAGE
BLACK AND WHITE PHOTOGRAPH

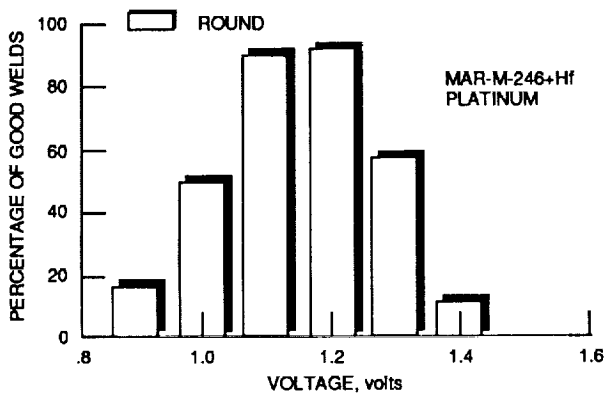


Figure 6. - Effect of weld voltage on weld quality for Pt-wire-to-Pt-film junctions on MAR-M-246+Hf superalloy substrates.

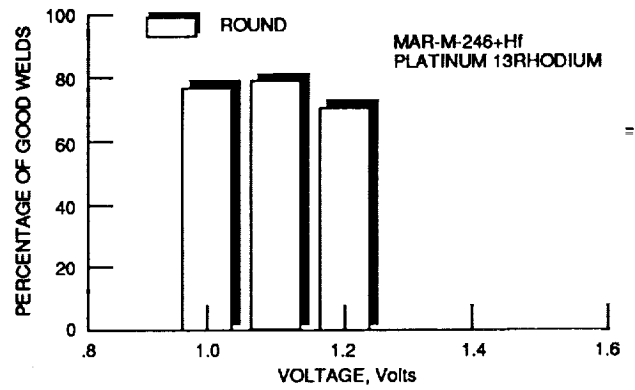


Figure 7. - Effect of weld voltage on weld quality for Pt13Rh-wire-to-Pt13Rh-film junctions on MAR-M-246+Hf superalloy substrates.

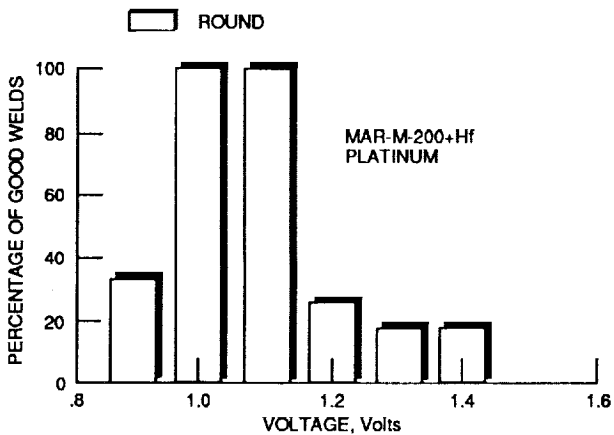


Figure 8. - Effect of weld voltage on weld quality for Pt-wire-to-Pt-film junctions on MAR-M-200+Hf superalloy substrates.

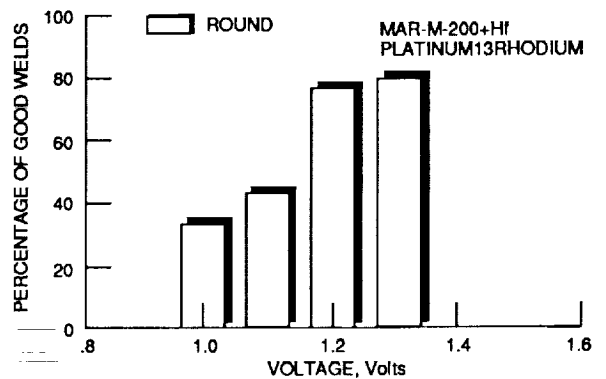


Figure 9. - Effect of weld voltage on weld quality for Pt13Rh-wire-to-Pt13Rh-film junctions on MAR-M-200+Hf superalloy substrates.

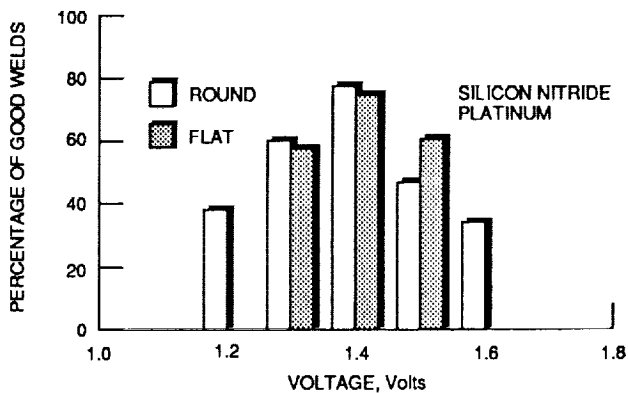


Figure 10. - Effect of weld voltage on weld quality for Pt-wire-to-Pt-film junctions on Silicon Nitride substrates.

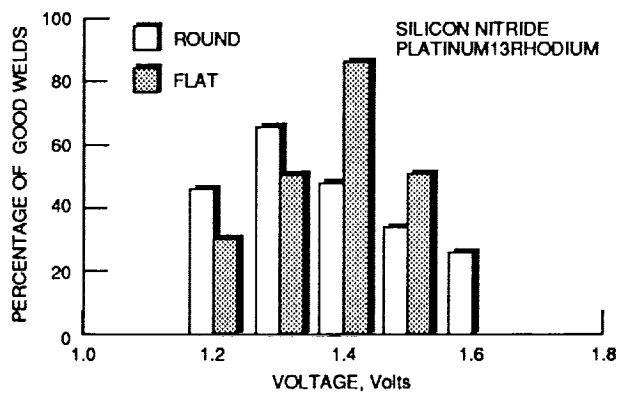


Figure 11. - Effect of weld voltage on weld quality for Pt13Rh-wire-to-Pt13Rh-film junctions on Silicon Nitride substrates.

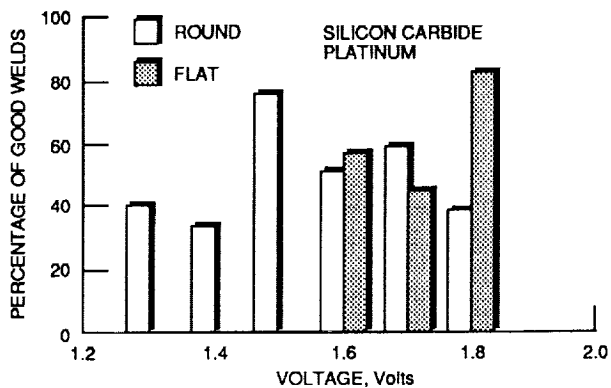


Figure 12. - Effect of weld voltage on weld quality for Pt-wire-to-Pt-film junctions on Silicon Carbide substrates.

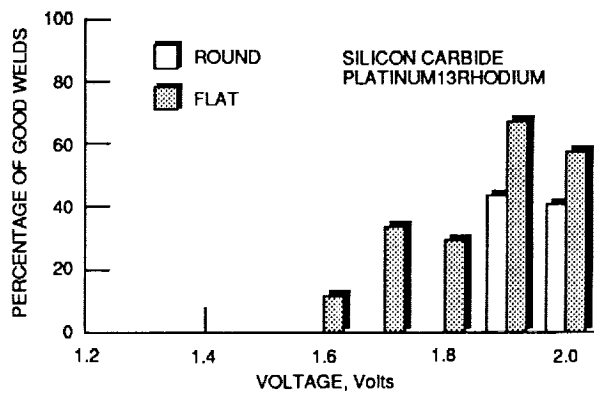


Figure 13. - Effect of weld voltage on weld quality for Pt13Rh-wire-to-Pt13Rh-film junctions on Silicon Carbide substrates.

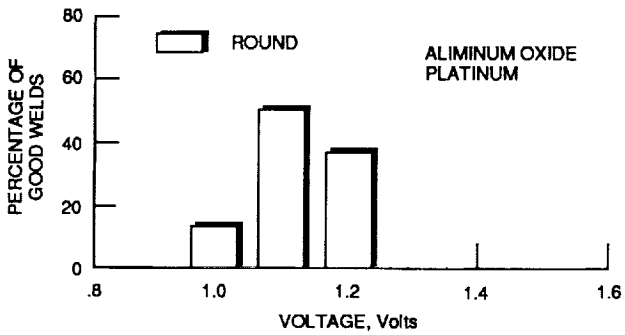


Figure 14. - Effect of weld voltage on weld quality for Pt-wire-to-Pt-film junctions on Aluminum Oxide substrates.

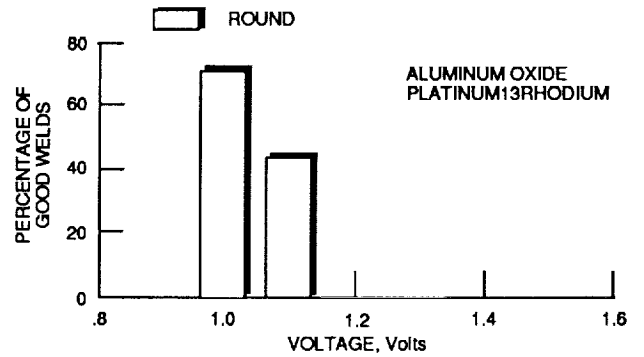


Figure 15. - Effect of weld voltage on weld quality for Pt13Rh-wire-to-Pt13Rh-film junctions on Aluminum Oxide substrates.

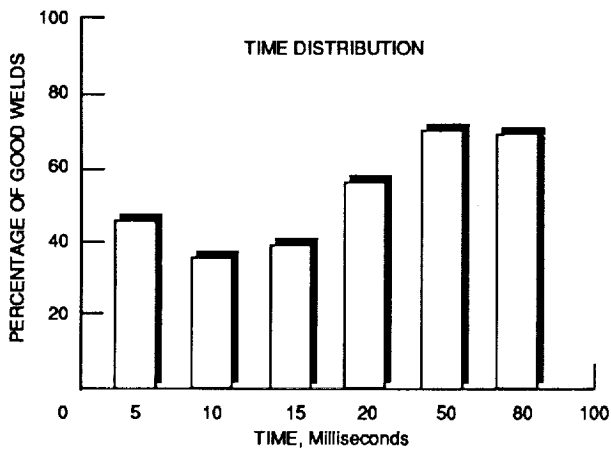


Figure 16. - Effect of weld time duration on weld quality for all thin-film-to-lead-wire junctions on all substrates.

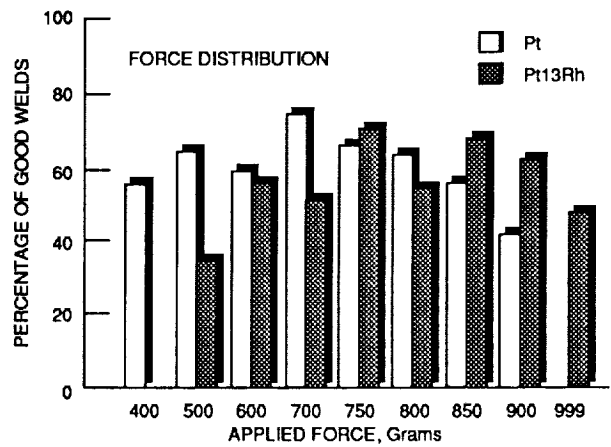


Figure 17. - Effect of applied electrode force on weld quality for all thin-film-to-lead-wire junctions on all substrates.

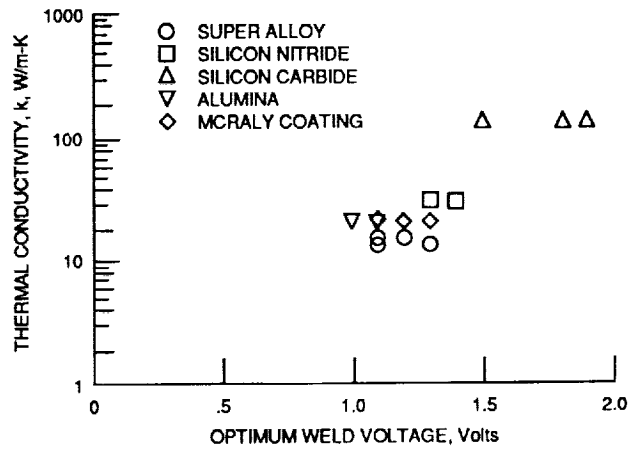
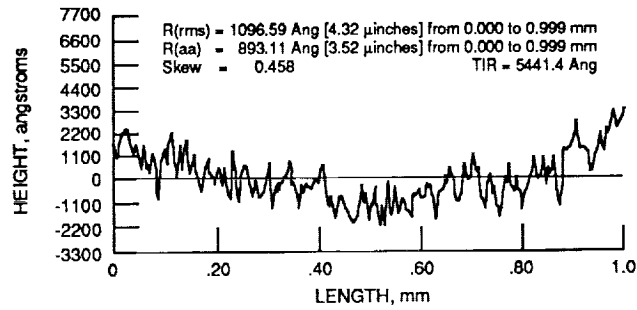
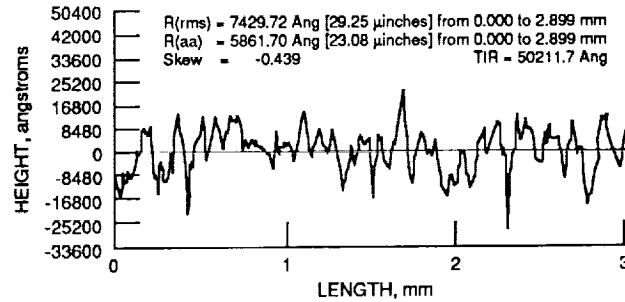


Figure 18. - Thermal conductivity of substrate vs optimum weld voltage required to obtain a successful weld on that substrate.



(a) Aluminum oxide.



(b) Mar-M-200+Hf.

Figure 19. - Stylus-type profilometer surface roughness profiles and R values for typical examples of Si_3N_4 , SiC, Al_2O_3 , and superalloy substrates.

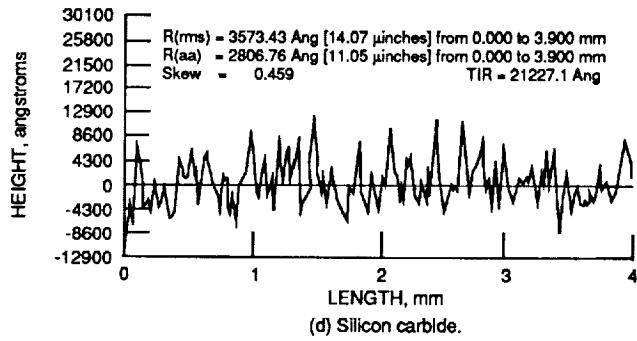
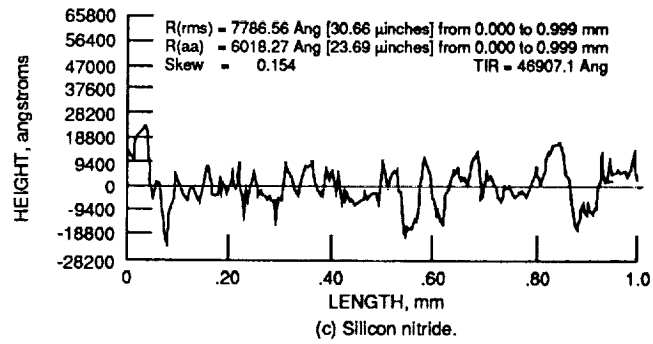


Figure 19. - Concluded.

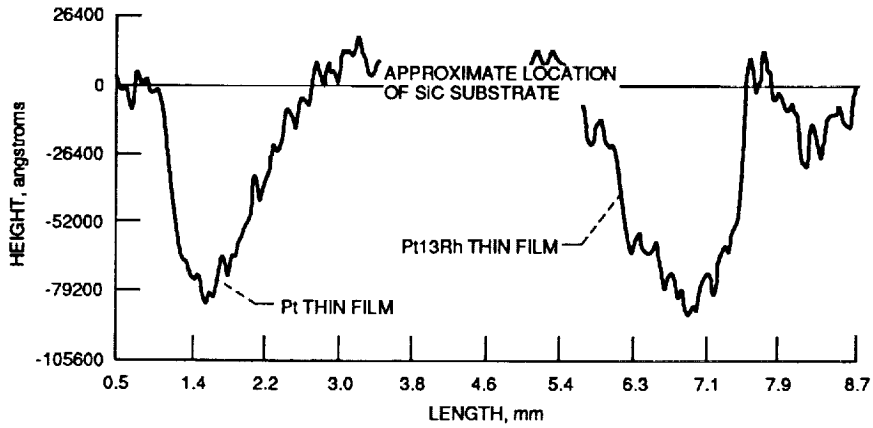


Figure 20. - Stylus-type profilometer film thickness profiles of Pt and Pt13Rh thin film on a SiC substrate.

1. Report No. NASA TM-102442		2. Government Accession No.		3. Recipient's Catalog No.	
4. Title and Subtitle Attachment of Lead Wires to Thin Film Thermocouples Mounted on High Temperature Materials Using the Parallel Gap Welding Process				5. Report Date	
				6. Performing Organization Code	
7. Author(s) Raymond Holanda, Walter S. Kim, Eric Pencil, Mary Groth, and Gerald A. Danzey				8. Performing Organization Report No. E-5218	
				10. Work Unit No. 510-01-0A	
9. Performing Organization Name and Address National Aeronautics and Space Administration Lewis Research Center Cleveland, Ohio 44135-3191				11. Contract or Grant No.	
				13. Type of Report and Period Covered Technical Memorandum	
12. Sponsoring Agency Name and Address National Aeronautics and Space Administration Washington, D.C. 20546-0001				14. Sponsoring Agency Code	
15. Supplementary Notes Prepared for the 177th Meeting of the Electrochemical Society, Montreal, Quebec, Canada, May 6-11, 1990. Raymond Holanda, Walter S. Kim and Gerald A. Danzey, NASA Lewis Research Center; Eric Pencil and Mary Groth, University of Cincinnati, Cincinnati, Ohio 45221 and Student Co-op at NASA Lewis Research Center.					
16. Abstract Parallel gap resistance welding was used to attach lead wires to sputtered thin film sensors. Ranges of optimum welding parameters to produce an acceptable weld were determined. The thin film sensors were Pt13Rh/Pt thermocouples; they were mounted on substrates of MCrAlY-coated superalloys, aluminum oxide, silicon carbide, and silicon nitride. The wires were 76 micrometer diameter Pt and Pt13Rh, and both round and preflattened wires were used. The entire sensor system is designed to be used on aircraft engine parts. These sensor systems, including the thin-film-to-lead-wire connections, have been tested to 1000 °C.					
17. Key Words (Suggested by Author(s)) Thin film; Sensor technology; Thermocouples; Welding; High temperature materials			18. Distribution Statement Unclassified - Unlimited Subject Category 35		
19. Security Classif. (of this report) Unclassified		20. Security Classif. (of this page) Unclassified		21. No. of pages 18	22. Price* A03